Parasitol Res (2013) 112:1719–1727
DOI 10.1007/s00436-013-3330-6

ORIGINAL PAPER

Identification and biochemical characterization of adenylate kinase 1 from *Clonorchis sinensis*

Pei Liang · Fan Zhang · Wenjun Chen · Xuchu Hu · Yan Huang · Shan Li · Mengyu Ren · Lei He · Ran Li · Xuerong Li · Jin Xu · Zhongdao Wu · Gang Lu · Xinbing Yu

Received: 6 November 2012 / Accepted: 29 January 2013 / Published online: 28 February 2013

Abstract Adenylate kinase 1 is responsible for the conversion of AMP into ADP involved in purine metabolism. In the present study, adenylate kinase 1 gene (*Cs*ADK1) was isolated from an adult cDNA library of *Clonorchis sinensis*, and the recombinant protein was expressed in *Escherichia coli*. Bioinformatics analysis implied that the putative protein contained 197 amino acids, and some residues in conservative binding sites of *Cs*ADK1 were substituted. The structure modeling analysis showed that *Cs*ADK1 was composed of a core domain, an NMP-binding domain, and a LID domain, which was just a small loop. It demonstrated that *Cs*ADK1 was a short isoform of ADKs. Moreover, *Cs*ADK1 was identified as an excretory/secretory product by western blot analysis. Real-time quantitative PCR showed that expression level of *Cs*ADK1 at the stage of excysted metacercaria was higher than those of adult worm (18.8-folds, $P<0.01$), metacercariae (1.5-folds, $P<0.01$), and eggs (5.6-folds, $P<0.01$). In addition, histochemistry analysis showed that *Cs*ADK1 was extensively distributed in metacercariae and in the vitellaria and eggs of adult worms. The K_m and V_{max} value for substrate ADP were 2.2 mM and 0.9 mM/min, respectively. The optimal temperature and pH value were 37 °C and from 7.5 to 8.0, respectively. The enzyme activity was highly dependent on Mg^{2+}, and the optimal concentration of Mg^{2+} was 2 mM. However, the enzyme activity was slightly activated by Ca^{2+}, and Mn^{2+} has no effect on activity. For monovalent ions, activity was highly activated by K^+ and NH_4^+, but slightly by Li^+. Taken together, *Cs*ADK1 was a metal ion-dependent enzyme involved in purine metabolism, which was important for development and reproduction, and might be a potential candidate for drug target for clonorchiasis.

Pei Liang and Fan Zhang contributed equally to this article.

P. Liang · F. Zhang · W. Chen · X. Hu · Y. Huang · S. Li · M. Ren · L. He · R. Li · X. Li · J. Xu · Z. Wu · X. Yu
Department of Parasitology, Zhongshan School of Medicine, Sun Yat-sen University, Guangzhou 510080, China

P. Liang · F. Zhang · W. Chen · X. Hu · Y. Huang · S. Li · M. Ren · L. He · R. Li · X. Li · J. Xu · Z. Wu · X. Yu (✉)
Key Laboratory for Tropical Diseases Control, Ministry of Education, Sun Yat-sen University, Guangzhou 510080, China
e-mail: yuhxteam@163.com

G. Lu (✉)
Department of Pathogen Biology, Hainan Medical College, Haikou, Hainan 571199, China
e-mail: luganghn@yahoo.com.cn

Introduction

Clonorchiasis, resulted from *Clonorchis sinensis* infection, is an important zoonosis and public health problem (Qiao et al. 2012; Huang et al. 2012). It mainly distributes in East Asia and Southeast Asia, including China and Korea (Rim 2005). People are infected with *C. sinensis* by consuming raw or undercooked freshwater fish containing metacercariae of *C. sinensis*. After entering the duodenum, metacercariae excyst and migrate into bile duct and develop into adults. Excretory/secretory products of *C. sinensis* adults (*Cs*ESPs) were generally considered to play a crucial role in host–parasite interactions (Kang et al. 2010a; Lv et al. 2012). Moreover, adult worms release a number of eggs into the gallbladder which induce the formation of gallbladder stone (Qiao et al. 2012). The infection of *C. sinensis* can result in serious liver and biliary system damages and, in chronic cases, may induce liver and bile duct cancers (Wu et al. 2012). However, it is essential to search for new therapeutic drugs for clonorchiasis control and to investigate important molecules for development and reproduction of *C. sinensis*.

Adenylate kinases (ADKs) are key enzymes in the energy metabolism of prokaryotic and eukaryotic cells (Bandlow et al. 1998), and the smallest phosphotransferases (Saint Girons et al. 1987). ADKs catalyze the reversible reaction of phosphoryl exchange between nucleotides ATP+AMP↔ 2 ADP and are regulated by availability of AMP or ADP (Zeleznikar et al. 1995) that is involved in metabolic energy and signaling pathway (Dzeja and Terzic 2009). Structurally, ADKs are composed of three domains: a core domain, containing a parallel β-sheet surrounded by α-helices; an NMP-binding domain, where the AMP binds; and a domain denominated LID, which is composed of residue segment (Fukami-Kobayashi et al. 1996). LID domain covers the nucleotides and locates in the middle part of the protein (Muller and Schulz 1992; Bouvier et al. 2006).

In vertebrates, there are five ADK isoforms (ADK1-5) with various substrate specificities and tissue distribution that have been found (Van Rompay et al. 2000). They can be divided into short isoform and long isoform with extra 27 amino acid residues in the LID domain (Schulz et al. 1986; Fukami-Kobayashi et al. 1996). Some vertebrate ADK isozymes such as ADK2 and ADK3 belong to the long isoform, whereas other vertebrate ADK isozymes such as ADK1 and ADK5 are the short isoform (Bouvier et al. 2006). AKDs are found in mitochondria, cytosol, and cellular membranes, creating an integrated phosphoryl transfer network (Dzeja et al. 1998; Elvir-Mairena et al. 1996; Tanabe et al. 1993), which is critical for the cell's life cycle. ADK1 localizes to the cytoplasm (Stanojevic et al. 2008). Tissues with great energy demand are particularly rich in ADK1, and ADK1-catalyzed phosphotransfer is essential in the maintenance of cellular energetic economy (Janssen et al. 2000). In *Schistosoma mansoni*, ADK1 plays a key role in the purine salvage pathway for energy and DNA biosynthesis (Marques Ide et al. 2012). ADK1 of *Plasmodium falciparum*, located in the cytosol, participates in energy transfer (Ma et al. 2012). ADK3 of *C. sinensis* was cloned, and its characteristics were analyzed (Yang et al. 2005). However, ADK1 has not been ever identified in *C. sinensis*. In the current study, *Cs*ADK1 gene was cloned, and the biochemical properties of recombinant *Cs*ADK1, immunolocalization, and transcriptional level of *Cs*ADK1 at different life stages of *C. sinensis* were characterized.

Materials and methods

Sequence analysis

The cDNA sequence encoding *Cs*ADK1 was obtained from a *C. sinensis* cDNA library according to previous description (Song et al. 2004), and the open reading frame (ORF) was found with ORF finder tool in NCBI web site (http://www.expasy.org/). The web site was also used to predict the physicochemical properties, the function domain in deduced amino acids, and structure modeling. The homology and phylogenetic tree were analyzed by bioinformatics analysis software Vector NTI suit 8.0.

Expression and purification

The ORF of *Cs*ADK1 was amplified by polymerase chain reaction (PCR) from the template isolated from the cDNA library of adult *C. sinensis*. Specific PCR primers were as follows: forward primer 5′-CTAC*GGATCC*TTCC*CG*ATGGCTGAC-3′ and reverse primer 5′-CGTT*CTCGAG*TGTGGCGTGTTT-3′. The amplification conditions were 94 °C for 45 s, 53 °C for 45 s and 72 °C for 1 min for 35 cycles, and 72 °C for 10 min in GeneAmp PCR System (TProfessional Standard Gradient, Biometra). The PCR product was purified and cloned into a prokaryotic expression vector pET-28a (+) (Novagen, Germany) that predigested with the same restrictive endonucleases. The recombinant plasmid was conformed by DNA sequencing and then transformed into *Escherichia coli* BL21 (DE3) (Promega, USA).

The bacterial cells containing recombinant pET-28a (+) plasmid was induced by 1 mM isopropyl-1-thio-β-galactopyranoside (IPTG, Sigma, USA) at 37 °C for 4 h. The bacterial cells were collected by centrifugation at 4 °C and sonicated on ice. Supernatant was collected, and recombinant protein was purified by His Bind Purification kit (Novagen, Germany) according to the manufacturer's instructions. The lysate of induced host bacteria and purified protein were subjected to 12 % sodium dodecyl sulfate polyacrylamide gel electrophoresis (SDS-PAGE). The concentration of purified recombinant protein was determined by using the BCA protein assay kit (Novagen, Germany).

Preparation for antiserum

To prepare anti-*Cs*ADK1 rat serum, recombinant *Cs*ADK1 (r*Cs*ADK1) was emulsified with complete Freund's adjuvant and subcutaneously immunized with 200 μg of protein for each rat at the first time. Subsequently, each rat was given 100 μg of protein (emulsified with equivalent incomplete Freund's adjuvant) for three booster injections at 2-week intervals. Antiserum was collected at 8 weeks. The antibody titer was determined by enzyme-linked immunosorbent assay (ELISA).

Western blot analysis

The *Cs*ESPs were collected from adult worms according to the method previously described (Hu et al. 2007). Adult worms or metacercariae were crushed and cleaned by

centrifugation at 10,000×*g* for 15 min at 4 °C to obtain the proteins in supernatant. The concentration of total proteins was determined using the BCA. The recombinant *Cs*ADK1 (3 μg/lane), *Cs*ESPs, and the total protein of adult worms and metacercariae (20 μg/lane, respectively) were resolved by 12 % SDS-PAGE and then immobilized onto polyvinylidene difluoride membrane. The membranes were blocked with 5 % (*w*/*v*) skim milk at room temperature for 2 h, and then incubated with primary antibody (anti-r*Cs*ADK1 rat serum, anti-His mouse serum, rat serum infected with *C. sinensis*, and naïve rat serum, respectively, 1:100 dilutions in 0.1 % BSA-PBS) overnight at 4 °C. After the washing procedures, the membranes were incubated with horseradish peroxidase (HRP)-conjugated goat anti-mouse IgG or HRP-conjugated goat anti-rat IgG (1:3,000 dilutions in 0.1 % BSA–PBS, ProteinTech Group, USA) for 1 h at RT. The results were detected by chemiluminescence (chemiluminescent HRP substrate, Millipore, USA).

Real-time quantitative PCR (qRT-PCR)

Adult worms, excysted metacercaria, metacercariae, and eggs were collected as described previously (Kang et al. 2010b; Na et al. 2008). Total RNA from parasites in four stages were extracted by Trizol methods (Invitrogen, Carlsbad, CA, USA) according to the manufacturer's instructions and quantitated by nucleic acid/protein analyzer (Beckman Coulter, USA) and agarose gel electrophoresis, respectively. Approximately 1 μg of total RNA was reversely transcribed to cDNA with reverse transcriptase kit (TakaRa, Dalian, China). The qRT-PCR based on SYBR-Green I fluorescence (TakaRa) was performed by using Roche LightCycler 480 (Switzerland). The sense and antisense PCR primers of *Cs*ADK1 (GenBank accession number: AAN03782.1) were as follows: 5′-AGTCTGTCCATGCCTTTGCG-3′ and 5′-TGTCATCCACCCGACCACTA-3′, respectively. RNA integrity was used.

C. sinensis β-actin as an internal control and primers used for β-actin (GenBank accession number: EU109284) were 5′-ACCGTGAGAAGATGACGCAGA-3′ and 5′-GCCAAGTCCAAACGAAGAATT-3′. Reactions were carried out under the following conditions: 95 °C for 30 s, 40 cycles of 95 °C for 5 s, and 60 °C for 20 s, with an incremental increase of 0.1 °C/s from 60 °C to 95 °C. PCR products were quantified by LC480 Software (Roche Light Cycler 480, Switzerland). The data were analyzed by using the $2^{-\Delta\Delta Ct}$ method (Livak and Schmittgen 2001). All assays were tested in triplicate and repeated three times.

Immunohistochemical localization

Adult worms and metacercariae of *C. sinensis* were fixed with 4 % paraformaldehyde, embedded with paraffin, and sliced into 3–5 μm in thickness. Sections of worms and metacercariae were deparaffinized with dimethylbenzene and rehydrated with graded ethanol series (100 %, 95 %, 85 %, and 75 %). Sections were blocked with normal goat serum for 2 h at RT and then incubated with the anti-r*Cs*ADK1 rat serum and naïve rat serum (1:200 dilutions) overnight at 4 °C. Naïve rat serum was employed as negative control. After washing three times with PBST (phosphate-buffered saline, PBS containing 0.05 % Tween-20), the sections were incubated with Cy3-conjugated AffiniPure goat anti-rat IgG (1:400 dilutions in 0.1 % BSA–PBS, Molecular Probe, USA) for 1 h at RT in dark, then imaged under fluorescence microscope (Axio Imager Z1, ZEISS).

Enzyme activity assays

Activity of r*Cs*ADK1 was measured using adenosine diphosphate (ADP, Sigma, USA) as substrate according to previous description (Milagros Camara Mde et al. 2012). The activity was determined spectrophotometrically by monitoring the rate of the reduction of $NADP^+$ to NADPH at 340 nm with a coupled enzyme assay. A sample of 3 μg per milliliter purified protein was added to the reaction mixture containing 100 mM Tris–HCl (pH7.5, Genebase, China), 20 mM glucose (Sigma, USA), 5 mM $MgCl_2$, 10 mM KCl, 2 mM dithiothreitol, 1 mM $NADP^+$, 5 units/ml hexokinase (Sigma, USA), and 2 units/ml glucose-6-phosphate dehydrogenase (Sigma, USA). After 5 min at 37 °C, the reactions were started by the addition of 10 mM ADP. The activity was calculated by measuring the increase in absorbance at 340 nm that accompanied with the reduction of $NADP^+$. All experiments were adapted to Michaelis–Menten equation $V = V_{max}[S]/(K_m + [S])$.

Statistical analysis

All experiments were repeated at least three times, and the data were presented as mean±SD and analyzed by one-way ANOVA using SPSS 12.0 software. The *p* value of less than 0.05 was considered statistically significant.

Results

Sequence analysis and structure modeling of *Cs*ADK1

The ORF of *Cs*ADK1 contained 594 base pairs (bp) encoding a protein of 197 amino acids (26.7 kDa with 12× His-tag). The deduced amino acid sequence shared 74 %, 73 %, 56 %, 55 %, and 52 % identity with ADK1 from *S. mansoni*, *Schistosoma japonicum*, *Mus musculus*, *Rattus norvegicus*, and *Homo sapiens*, respectively (Fig. 1). The amino acids forming the canonic phosphoryl loop (P-loop) were

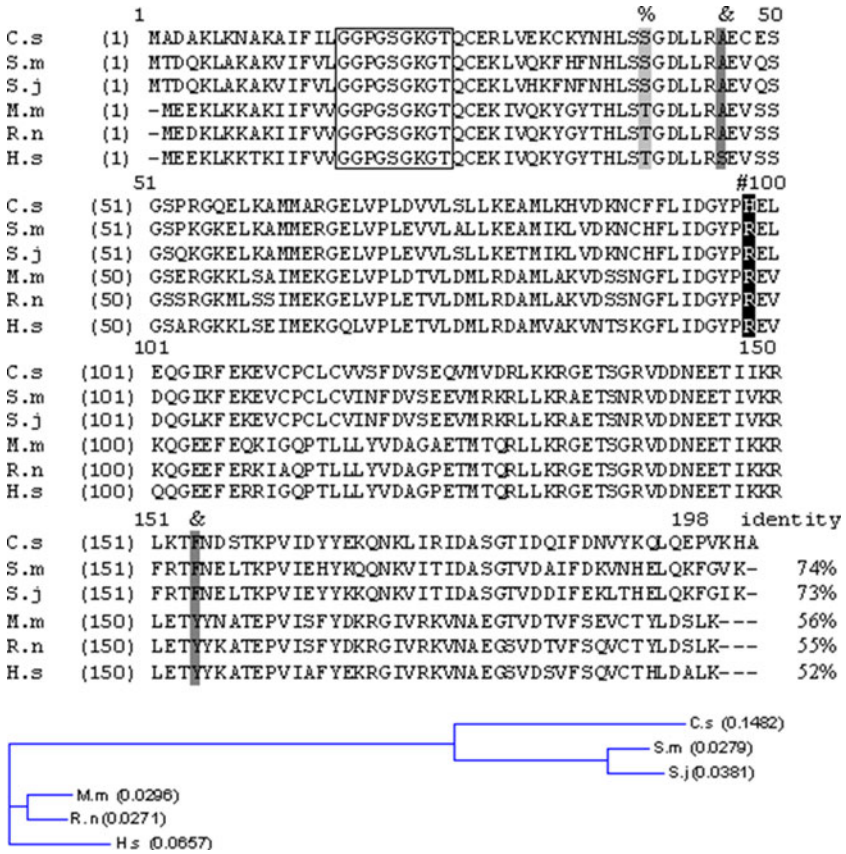

Fig. 1 **a** Alignment of the deduced amino acid sequence of *Clonorchis sinensis* adenylate kinase 1 (*C. sinensis*, GenBank Accession No. AAN03782.1) with other adenylate kinase 1 sequences: *Schistosoma mansoni* (*S. mansoni*, GenBank Accession No. XP_002578326.1), *Schistosoma japonicum* (*S. japonicum*, GenBank Accession No. CAX75422.1), *Mus musculus* (*M. musculus*, GenBank Accession No. NP_001185719.1), *Rattus norvegicus* (*R. norvegicus*, GenBank Accession No. BAA97655.1), and *Homo sapiens* (*H. sapiens*, GenBank Accession No. NP000467.1). The conservative substitution was *shaded in gray* with *percent symbol*, *ampersand*, and *number sign*. *Percent symbol*: substitution in ATP–AMP binding sites. *Ampersand*: substitution in AMP binding sites. *Number sign*: substitution in the overlaps of ATP–AMP binding sites and AMP binding sites. The amino acids forming the canonic phosphoryl loop (P-loop, GxxGxGxxT) were demonstrated with a *frame*. **b** The phylogenetic tree of ADK1

demonstrated with a frame. Comparisons with the AMP and ATP binding sites of ADK1 from mammalian (*M. musculus*, *R. norvegicus*, and *H. sapiens*) showed only one substitution S40T (T39 in mammalian ADK1). Moreover, there were two substitutions of A46S and F154Y in the AMP binding sites (S45 and Y153 in human ADK1, respectively). Furthermore, there was one substitution: H98R (R98 or R97 in other species) in the overlaps by the AMP and ATP

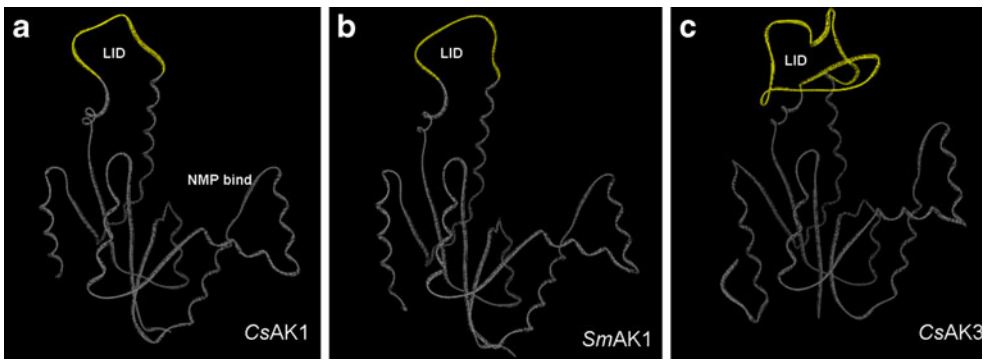

Fig. 2 Three-dimensional structure of ADK1 Ribbon presentation. **a** The three-dimensional structure of *Cs*ADK1 Ribbon presentation. **b** The three-dimensional structure of *Sm*ADK1 Ribbon presentation. **c** The three-dimensional structure of *Cs*ADK3 Ribbon presentation. The conserved domains of ADK1 were a core domain, containing a parallel β-sheet surrounded by α-helices; an NMP-binding domain; and a LID domain, which converts the nucleotides. Compared with the LID domain of *Cs*ADK3, *Cs*ADK1 has a small loop

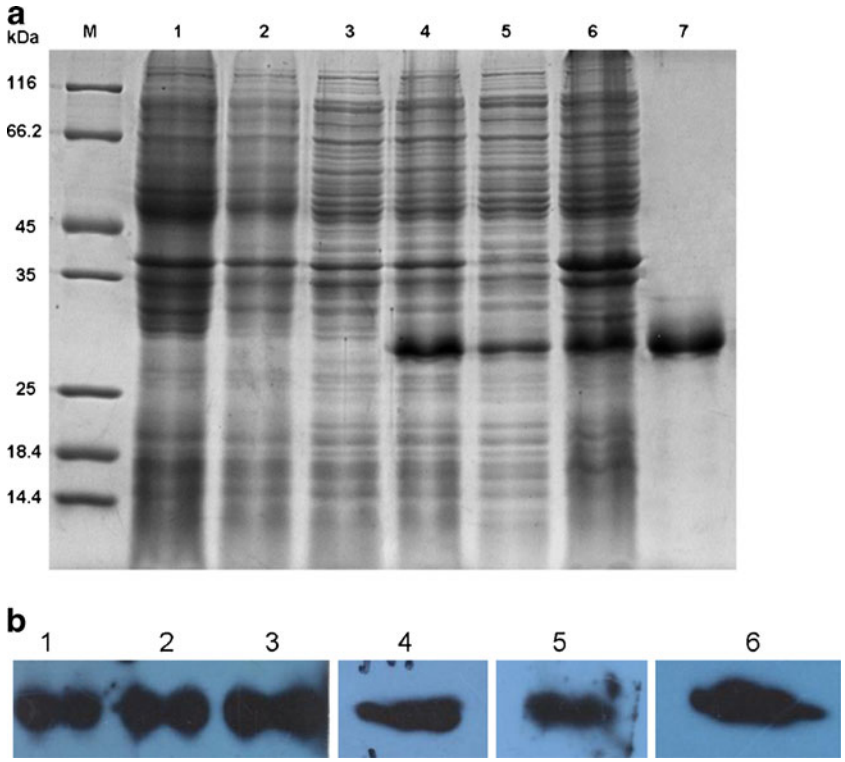

Fig. 3 **a** Expression and purification of r*Cs*ADK1 by 12 % SDS-PAGE. Protein molecular weight markers (*lane M*), lysate of *Escherichia coli* with pET-28a (+) before induction (*lane 1*) and after induction (*lane 2*), lysate of *E. coli* with pET28a (+)-*Cs*ADK1 before induction (*lane 3*) and after induction (*lane 4*), supernatant (*lane 5*) and precipitant (*lane 6*) of lysate of *E. coli* with pET28a (+)-*Cs*ADK1 after induction (*lane 7*), and the purified recombinant *Cs*ADK1 protein. **b** Identification of *Cs*ADK1 as a component of *Cs*ESPs. r*Cs*ADK1 protein was immobilized and probed with anti-r*Cs*ADK1 rat serum, anti-His-tag mouse serum, and *Clonorchis sinensis*-infected rat serum (*lanes 1–3*, respectively). The total extracts of adult worms and metacercariae were probed by anti-r*Cs*ADK1 rat serum, respectively (*lanes 4* and *5*, respectively). *Cs*ESPs were probed with anti-r*Cs*ADK1 rat serum (*lane 6*). The naïve serum was as control

binding sites and the AMP binding sites. A phylogenetic tree was constructed based on multiple ADK1 sequences from various species in Fig. 1. *Cs*ADK1 was composed of a core domain, an NMP-binding domain, and a LID domain, which was just a small loop (Fig. 2).

Expression and purification of r*Cs*ADK1

The soluble r*Cs*ADK1 was expressed with 12× His-tag in *E. coli* BL21 after being induced by 1 mM IPTG at 37 °C for 4 h. The molecular mass of purified protein was about 26.7 kDa (Fig. 3a), and the final protein concentration was 10 mg/L.

Identification of *Cs*ADK1 as a component of *Cs*ESPs

Purified r*Cs*ADK1 could react with anti-r*Cs*AK1 rat serum, anti-His mouse serum, and rat serum infected with *C. sinensis* (Fig. 3b, lanes 1–3, respectively) at 26.7 kDa. The total extracts of adult worms and metacercariae and *Cs*ESPs were probed by anti-r*Cs*ADK1 rat serum (Fig. 3b, lanes 4–6). However, no band was detected by naïve rat serum (not shown).

Transcriptional level at different developmental stages

The result was calculated according to the previous methods (Livak and Schmittgen 2001). As shown in Fig. 4,

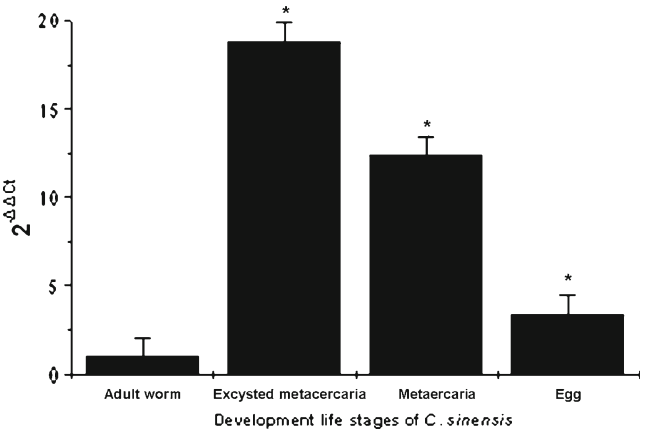

Fig. 4 Real-time quantitative assay of *Cs*ADK1 at different life stages of *Clonorchis sinensis*. *y*-axis represents the level of quantitative mRNA at life stages. Expression level of *Cs*ADK1 at the stage of excysted metacercariae was higher than that of adult worms (18.76-folds, $P<0.01$), metacercariae (1.52-folds, $P<0.01$), and eggs (5.62-folds, $P<0.01$)

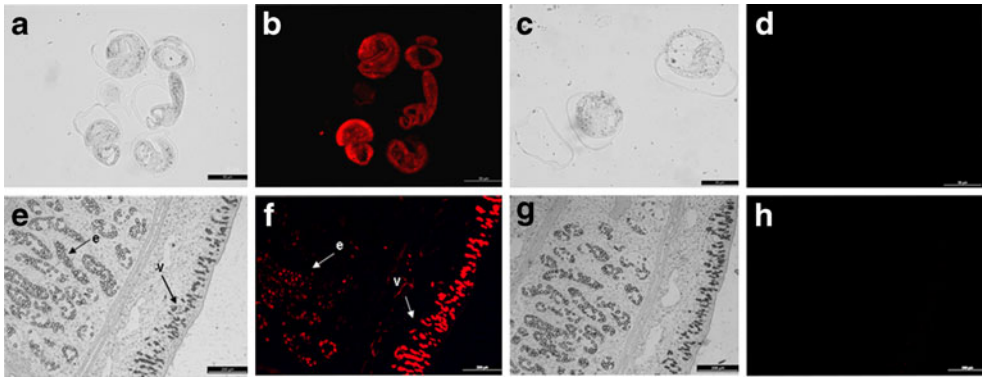

Fig. 5 Immunolocalization of *Cs*ADK1 in *Clonorchis sinensis* metacercariae and adult worms. *Cs*ADK1 was extensively distributes in metacercariae (**b**). In the adult worms, *Cs*ADK1 was localized in the vitellaria and eggs (**f**). Negative controls were carried out with naïve serum (1:100 *v*/*v* dilutions) for metacercariae (**d**) and for adult worms (**h**). **a**, **c** Corresponding bright fields for metacercariae. **e**, **g** Corresponding bright fields for the adult worms. The images were magnified at ×100 for adult worms and ×400 for metacercariae, respectively. *v* vitellaria, *e* eggs

transcriptional level of *Cs*ADK1 was detected at the life stages of adult worms, excysted metacercaria, metacercariae, and eggs of *C. sinensis*. Obviously, it showed that transcriptional level of *Cs*ADK1 at the stage of excysted metacercaria was higher than that of adult worm (18.8-folds, $P<0.01$), metacercariae (1.5-folds, $P<0.01$), and eggs (5.6-folds, $P<0.01$).

Immunohistochemical localization of *Cs*ADK1

Figure 5 showed that *Cs*ADK1 was extensively distributed in metacercariae (Fig. 5b) and in the vitellaria and eggs of adult worms (Fig. 5f). No specific fluorescence was detected either in adult worms or in metacercariae when treated with naïve mouse serum (Fig. 5d, h).

Enzymatic assays

The K_m and V_{max} value of *Cs*ADK1 was 2.2 mM and 0.9 mM/min when using ADP as substrate in this coupled enzyme assay, respectively (Fig. 6). Enzyme activity of r*Cs*ADK1 maintained more than 50 % of maximal activity between 30 °C and 50 °C, and the optimal temperature was 37 °C (not shown). The activity was weak when pH value was under 6.0 and up to 60 % of maximal activity when pH value was 10.0. The optimal pH value was from 7.5 to 8.0 (not shown). The activity was increasing with varied concentrations of Mg^{2+} from 1 to 5 mM. However, it changed a little when the concentration was up to 10 mM. The optimal concentration of Mg^{2+} for the enzyme activity was 2 mM (Fig. 7a). The effect of K^+ on enzyme activity was detected, and the optimal concentration was 10 mM (Fig. 7b). Table 1 showed that the enzyme activity was increasing in the order $Mg^{2+}>Ca^{2+}>Mn^{2+}$. In the effect of monovalent ions on enzyme activity, it was highly activated by K^+ and NH_4^+, but slightly by Li^+ compared with control.

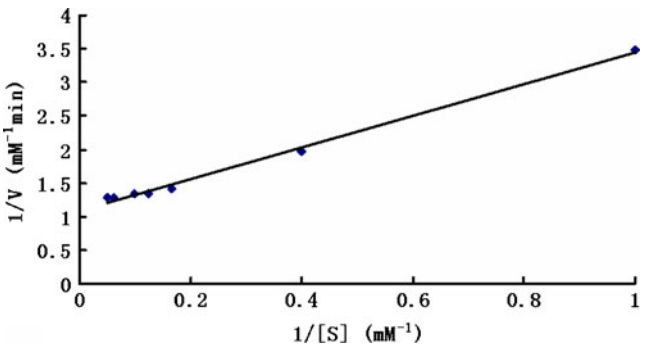

Fig. 6 To determine value of the K_m and V_{max} of r*Cs*ADK1, the reaction was detected. Lineweaver–Burk double reciprocal plot of r*Cs*ADK1

Discussion

Our genome and transcriptome data of *C. sinensis* showed enzymes involved in purine metabolism and pyrimidine metabolism (Wang et al. 2011a). However, enzymes which participated in de novo purine nucleotide synthesis were absent in the parasite. On the contrary, enzymes involved in salvage pathway were expressed, such as adenine phosphoribosyltransferase and hypoxanthine phosphoribosyltransferase. It suggested that salvage pathway was present in *C. sinensis*. In the *S. mansoni*, it totally depends on the purine salvage pathway in order to supply large quantities of purine precursors for its energy and DNA biosynthesis (Marques Ide et al. 2012), while ADK1 has participated in salvage pathway to provide purine nucleotides for *S. mansoni* (Marques Ide et al. 2012). It is possible that *C. sinensis* may obtain purine precursors for energy and DNA biosynthesis by ADK1 because ADK1 is involved in the homeostasis of adenine nucleotides by interconversion of constituents of the adenine

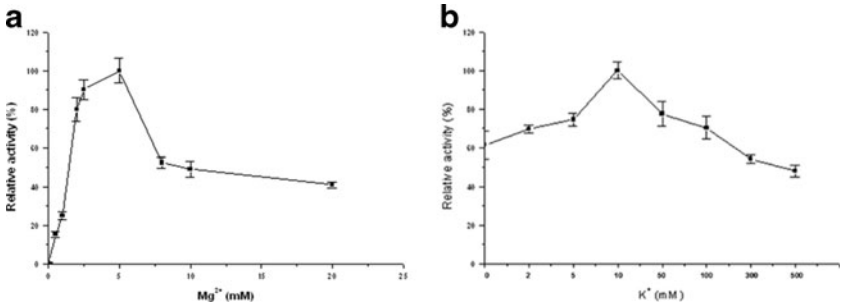

Fig. 7 Enzymatic characteristics of r*Cs*ADK1 were detected. **a** Effects of Mg^{2+} on r*Cs*ADK1 activity was detected. **b** Effects of K^{+} on r*Cs*ADK1 activity was detected

nucleotide pool and duplicating the ATP energetic potential via its synthesis from ADP (Schulz et al. 1986; Janssen et al. 2000; Ma et al. 2012).

In the present study, we first identified an isoform enzyme of ADKs and characterized the structures and biochemical properties of *Cs*ADK1. The conservative binding sites of *Cs*ADK1 were substituted for other residues. This conservative substitution is observed in other ADK1, such as ADK1 from *S. mansoni* and *S. japonicum* (Marques Ide et al. 2012). *Cs*ADK1 had the P-loop with the conservative residues GxxGxGxxT. *Cs*ADK1 was a short isoform, and the LID domain was just a small loop as similar in *Sm*ADK1 (Marques Ide et al. 2012). It was obviously different with *Cs*ADK3 containing four β-strands (Fig. 2c). In addition, a novel gene ADK1 of *C. sinensis* was cloned, and the protein was expressed. It is a soluble protein (Fig. 3a) that paves the way for further functional research.

The transcriptional level of *Cs*ADK1 was detected in all developmental stages of *C. sinensis*. *Cs*ADK1 were intensively expressed in vitellaria and eggs of adult worms but distributed extensively in metacercariae, indicating it is actively involved in development and reproduction of *C. sinensis*. In the enzymatic activity assay, the K_m and V_{max} value of *Cs*ADK1 was 2.2 mM and 0.9 mM/min when using ADP as substrate, respectively. Upon ligand binding, the enzyme undergoes a transition from the inactive open form to the catalytically competent closed structure according to the analysis of the crystal structures (Vonrhein et al. 1995). This transition is mediated by large-scale closure motions of the LID and AMP domains insulating the substrates from the water environment, while occluding some catalytically relevant water molecules (Matsunaga et al. 2012). The kinetic properties of *Cs*ADK1 showed that optimal pH value is 7.5 to 8.0, the normal pH scope of bile. However, the enzyme of *Tritrichomonas foetus* has a broad optimal pH range between 6.0 and 9 (Dinbergs and Lindmark 1989). In other words, *Cs*ADK1 was an acid-sensitive enzyme and insensitive to alkaline environment. When metacercariae excyst and migrate into bile duct and develop into adults, *Cs*ADK1 maintained its functions in energy supply and the homeostasis of adenine nucleotides. Moreover, Mg^{2+} was essential for activity of *Cs*ADK1 (Bouvier et al. 2006), while Mn^{2+} had little effects on it. On the contrary, in *T. foetus*, full enzyme activity requires Mg^{2+}, but Mn^{2+} can yield half maximal activity (Dinbergs and Lindmark 1989). It demonstrated that *Cs*ADK1 was an Mg^{2+}-dependent enzyme. The activity was obviously activated at the low concentration of K^{+}. In Table 1, the effect of $NH4^{+}$ on activity was the same as K^{+}, but was slightly activated by Li^{+}. Taken together, it could help to explain the slight difference in the kinetic parameters when compared with their mammalian counterpart. Moreover, the presence of different residues in the binding sites opens up the possibility of designing specific competitive inhibitors, which has a lower affinity for the human ortholog, for chemotherapy of clonorchiasis.

Western blotting (Fig. 3b) demonstrated that *Cs*ADK1 was one component of total proteins of adult worms and metacercariae of *C. sinensis*. Moreover, *Cs*ADK1 could react with rat serum infected with *C. sinensis*. It is implied that *Cs*ADK1 was also a circulating antigen which might derive from eggs of parasites. Furthermore, *Cs*ADK1 was identified as a component of *Cs*ESPs (Fig. 3b, lane 6). Interestingly, *Cs*ESPs may derive from the excoriation of parasites and excretion through intestine from parasites (Wang et al. 2011b). *Cs*ADK1 was relatively highly expressed in eggs of adult worm. It is possible that eggs are released from adult worms into bile duct, and excoriation or excretion of eggs may also be one of the sources of

Table 1 Effect of metal ions on the enzyme activity

Divalent metal ions	Concentration (mM)	Relative activity (%)	Monovalent metal	Concentration (mM)	Relative activity (%)
None	0	0	None	0	61.32±7.01
$MgCl_2$	5	100±9.95	KCl	10	100±6.84
$MnCl_2$	5	0	NH_4Cl	10	93.60±2.16
$CaCl_2$	5	0.85±0.25	LiCl	10	65.87±1.74

The data was repeated in triplicate and reflected the mean relative activity±SD

*Cs*ESPs. Moreover, qPCR results showed that transcriptional level of *Cs*ADK1 at the excysted metacercariae stage was the highest at these life stages. In the process of growth from metacercariae to adult worms, substantial energy and adenine nucleotides requirements must be met during this transformation. Taken together, *Cs*ADK1 may play a key role in energy supply and regulation of adenine nucleotides for excysted metacercariae stage of *C. sinensis*. The results of transcriptional level of *Cs*ADK1 were in accordance with immunolocalization at the metacercariae and eggs stages. In many organisms, energetic homeostasis is maintained by remodeling the phosphotransfer network. In mammals, the suppression of the adenylate kinase gene is complemented by glycolytic enzymes (Janssen et al. 2000, 2003; Dzeja et al. 2004). The transcriptional level of *Cs*ADK1 was less at adult worms. Moreover, three key enzymes involved in anaerobic glycolysis expressed higher in the stage (unpublished data). It is possible that the downregulation of *Cs*ADK1 is complemented by glycolytic enzymes in this stage.

In summary, we have identified a novel *Cs*ADK1 gene from the cDNA library of *C. sinensis*, expressed, and characterized the properties of the protein. In the bioinformatics analysis, *Cs*ADK1 had some differences from human ADK1 in conservative binding sites, and enzymatic characteristics were illustrated, indicating that it contributes to designing specific competitive inhibitors for clonorchiasis control. In addition, we demonstrated that it was a component of *Cs*ESPs from excoriation or excretion of eggs that was one of the sources of *Cs*ESPs. In other organisms, ADK1 is involved in a broad variety of cellular functions; however, in *C. sinensis*, most of the metabolic processes associated with *Cs*ADK1 remain unknown and require further investigation.

Acknowledgments This work was supported by the National Key Basic Research and Development Project of China (973 project; No. 2010CB530000), National Natural Science Foundation of China (No. 81101270 and No. 81171602), China Postdoctoral Science Foundation (No. 20110490952), and Fundamental Research Funds for the Central Universities. (No. 3164015).

References

Bandlow W, Strobel G, Schricker R (1998) Influence of N-terminal sequence variation on the sorting of major adenylate kinase to the mitochondrial intermembrane space in yeast. Biochem J 329 (2):359–367

Bouvier LA, Miranda MR, Canepa GE, Alves MJ, Pereira CA (2006) An expanded adenylate kinase gene family in the protozoan parasite *Trypanosoma cruzi*. Biochim Biophys Acta 1760 (6):913–921

Dinbergs ID, Lindmark DG (1989) *Tritrichomonas foetus*: purification and characterization of hydrogenosomal ATP:AMP phosphotransferase (adenylate kinase). Exp Parasitol 69(2):150–156

Dzeja PP, Terzic A (2009) Adenylate kinase and AMP signaling networks: metabolic monitoring, signal communication and body energy sensing. Int J Mol Sci 10(4):1729–1772

Dzeja PP, Terzic A, Wieringa B (2004) Phosphotransfer dynamics in skeletal muscle from creatine kinase gene-deleted mice. Mol Cell Biochem 256–257(1–2):13–27

Dzeja PP, Zeleznikar RJ, Goldberg ND (1998) Adenylate kinase: kinetic behavior in intact cells indicates it is integral to multiple cellular processes. Mol Cell Biochem 184(1–2):169–182

Elvir-Mairena JR, Jovanovic A, Gomez LA, Alekseev AE, Terzic A (1996) Reversal of the ATP-liganded state of ATP-sensitive K+ channels by adenylate kinase activity. J Biol Chem 271 (50):31903–31908

Fukami-Kobayashi K, Nosaka M, Nakazawa A, Go M (1996) Ancient divergence of long and short isoforms of adenylate kinase: molecular evolution of the nucleoside monophosphate kinase family. FEBS Lett 385(3):214–220

Huang Y, Li W, Huang L, Hu Y, Chen W, Wang X, Sun J, Liang C, Wu Z, Li X, Xu J, Yu X (2012) Identification and characterization of myophilin-like protein: a life stage and tissue-specific antigen of *Clonorchis sinensis*. Parasitol Res 111(3):1143–1150

Hu F, Yu X, Ma C, Zhou H, Zhou Z, Li Y, Lu F, Xu J, Wu Z, Hu X (2007) *Clonorchis sinensis*: expression, characterization, immunolocalization and serological reactivity of one excretory/secretory antigen-LPAP homologue. Exp Parasitol 117(2):157–164

Janssen E, de Groof A, Wijers M, Fransen J, Dzeja PP, Terzic A, Wieringa B (2003) Adenylate kinase 1 deficiency induces molecular and structural adaptations to support muscle energy metabolism. J Biol Chem 278(15):12937–12945

Janssen E, Dzeja PP, Oerlemans F, Simonetti AW, Heerschap A, de Haan A, Rush PS, Terjung RR, Wieringa B, Terzic A (2000) Adenylate kinase 1 gene deletion disrupts muscle energetic economy despite metabolic rearrangement. EMBO J 19(23):6371–6381

Kang JM, Bahk YY, Cho PY, Hong SJ, Kim TS, Sohn WM, Na BK (2010a) A family of cathepsin F cysteine proteases of *Clonorchis sinensis* is the major secreted proteins that are expressed in the intestine of the parasite. Mol Biochem Parasitol 170(1):7–16

Kang JM, Sohn WM, Ju JW, Kim TS, Na BK (2010b) Identification and characterization of a serine protease inhibitor of *Clonorchis sinensis*. Acta Trop 116(2):134–140

Livak KJ, Schmittgen TD (2001) Analysis of relative gene expression data using real-time quantitative PCR and the 2(−Delta Delta C (T)) method. Methods 25(4):402–408

Lv X, Chen W, Wang X, Li X, Sun J, Deng C, Men J, Tian Y, Zhou C, Lei H, Liang C, Yu X (2012) Molecular characterization and expression of a cysteine protease from *Clonorchis sinensis* and its application for serodiagnosis of clonorchiasis. Parasitol Res 110(6):2211–2219

Ma J, Rahlfs S, Jortzik E, Schirmer RH, Przyborski JM, Becker K (2012) Subcellular localization of adenylate kinases in *Plasmodium falciparum*. FEBS Lett 586(19):3037–3043

Marques Ide A, Romanello L, Demarco R, Pereira HD (2012) Structural and kinetic studies of *Schistosoma mansoni* adenylate kinases. Mol Biochem Parasitol 185(2):157–160

Matsunaga Y, Fujisaki H, Terada T, Furuta T, Moritsugu K, Kidera A (2012) Minimum free energy path of ligand-induced transition in adenylate kinase. PLoS Comput Biol 8(6):e1002555

Milagros Camara Mde L, Bouvier LA, Miranda MR, Pereira CA (2012) Identification and validation of *Trypanosoma cruzi*'s glycosomal adenylate kinase containing a peroxisomal targeting signal. Exp Parasitol 130(4):408–411

Muller CW, Schulz GE (1992) Structure of the complex between adenylate kinase from *Escherichia coli* and the inhibitor Ap5A refined at 1.9 A resolution. A model for a catalytic transition state. J Mol Biol 224(1):159–177

Na BK, Kang JM, Sohn WM (2008) CsCF-6, a novel cathepsin F-like cysteine protease for nutrient uptake of *Clonorchis sinensis*. Int J Parasitol 38(5):493–502

Qiao T, Ma RH, Luo XB, Luo ZL, Zheng PM (2012) Cholecystolithiasis is associated with *Clonorchis sinensis* infection. PLoS One 7(8):e42471

Rim HJ (2005) Clonorchiasis: an update. J Helminthol 79(3):269–281

Saint Girons I, Gilles AM, Margarita D, Michelson S, Monnot M, Fermandjian S, Danchin A, Barzu O (1987) Structural and catalytic characteristics of *Escherichia coli* adenylate kinase. J Biol Chem 262(2):622–629

Schulz GE, Schiltz E, Tomasselli AG, Frank R, Brune M, Wittinghofer A, Schirmer RH (1986) Structural relationships in the adenylate kinase family. Eur J Biochem 161(1):127–132

Song L, Chen S, Yu X, Wu Z, Xu J, Yang G, Zheng N, Hu X, Guo L, Dai J, Xu J, Ji C, Gu S, Ying K (2004) Molecular cloning and characterization of cDNA encoding a ubiquitin-conjugating enzyme from *Clonorchis sinensis*. Parasitol Res 94(3):227–232

Stanojevic V, Habener JF, Holz GG, Leech CA (2008) Cytosolic adenylate kinases regulate K-ATP channel activity in human beta-cells. Biochem Biophys Res Commun 368(3):614–619

Tanabe T, Yamada M, Noma T, Kajii T, Nakazawa A (1993) Tissue-specific and developmentally regulated expression of the genes encoding adenylate kinase isozymes. J Biochem 113(2):200–207

Van Rompay AR, Johansson M, Karlsson A (2000) Phosphorylation of nucleosides and nucleoside analogs by mammalian nucleoside monophosphate kinases. Pharmacol Ther 87(2–3):189–198

Vonrhein C, Schlauderer GJ, Schulz GE (1995) Movie of the structural changes during a catalytic cycle of nucleoside monophosphate kinases. Structure 3(5):483–490

Wang X, Chen W, Huang Y, Sun J, Men J, Liu H, Luo F, Guo L, Lv X, Deng C, Zhou C, Fan Y, Li X, Huang L, Hu Y, Liang C, Hu X, Xu J, Yu X (2011a) The draft genome of the carcinogenic human liver fluke *Clonorchis sinensis*. Genome Biol 12(10):R107

Wang X, Chen W, Hu F, Deng C, Zhou C, Lv X, Fan Y, Men J, Huang Y, Sun J, Hu D, Chen J, Yang Y, Liang C, Zheng H, Hu X, Xu J, Wu Z, Yu X (2011b) *Clonorchis sinensis* enolase: identification and biochemical characterization of a glycolytic enzyme from excretory/secretory products. Mol Biochem Parasitol 177(2):135–142

Wu W, Qian X, Huang Y, Hong Q (2012) A review of the control of *clonorchiasis sinensis* and *Taenia solium taeniasis*/*cysticercosis* in China. Parasitol Res 111(5):1879–1884

Yang G, Yu X, Wu Z, Xu J, Song L, Zhang H, Hu X, Zheng N, Guo L, Xu J, Dai J, Ji C, Gu S, Ying K (2005) Molecular cloning and characterization of a novel adenylate kinase 3 gene from *Clonorchis sinensis*. Parasitol Res 95(6):406–412

Zeleznikar RJ, Dzeja PP, Goldberg ND (1995) Adenylate kinase-catalyzed phosphoryl transfer couples ATP utilization with its generation by glycolysis in intact muscle. J Biol Chem 270(13):7311–7319